Ladder-Like Heteropolynuclear Assemblies via Cyanido Bridges and Platinum(II)-Thallium(I) Bonds: Structural and Photophysical Properties

Mina Sadeghian,[a,b] David Gómez de Segura,[b] Mohsen Golbon Haghighi,*[,a] Nasser Safari,[a] Elena Lalinde*[,b] and M. Teresa Moreno*[,b]

[a] Department of Chemistry, Shahid Beheshti University, Evin, Tehran 19839-69411, Iran. E-mail: m_golbon@sbu.ac.ir

[b] Departamento de Química, Instituto de Investigación en Química (IQUR), Complejo Científico Tecnológico, Universidad de La Rioja, 26006 Logroño, Spain. E-mail: elena.lalinde@unirioja.es; teresa.moreno@unirioja.es

1.- NMR Spectra S2
2.- Crystal Structures S8
3. Photophysical Properties and Theoretical Calculations S12

1.- NMR Spectra

a)

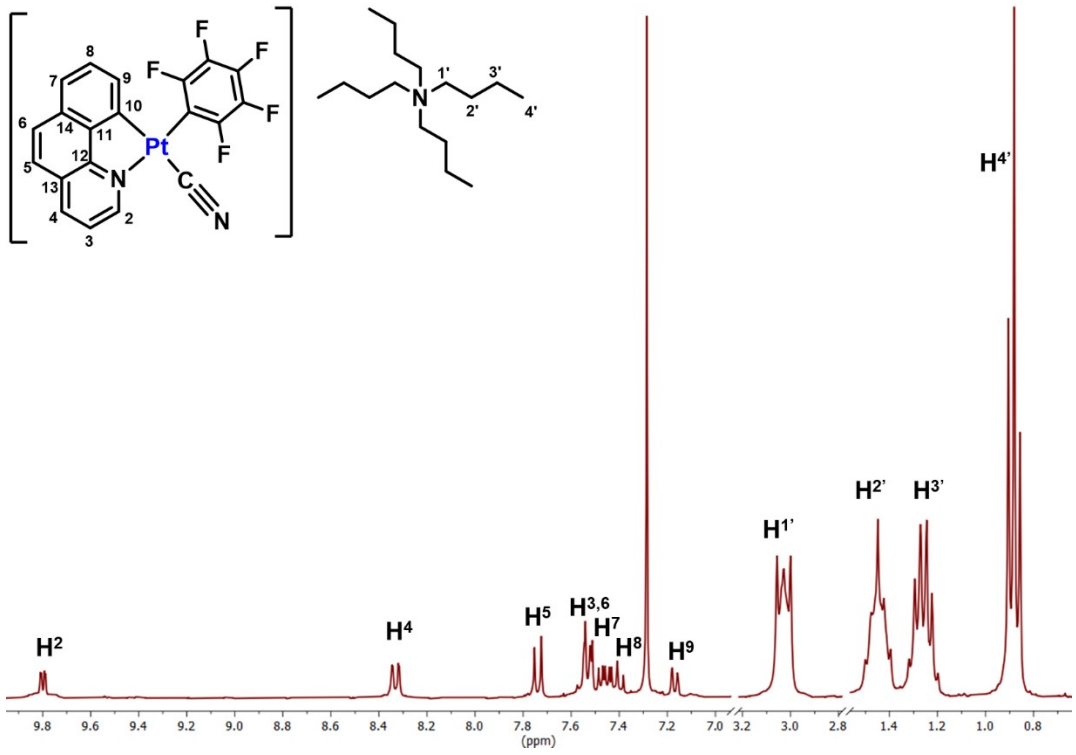

b)

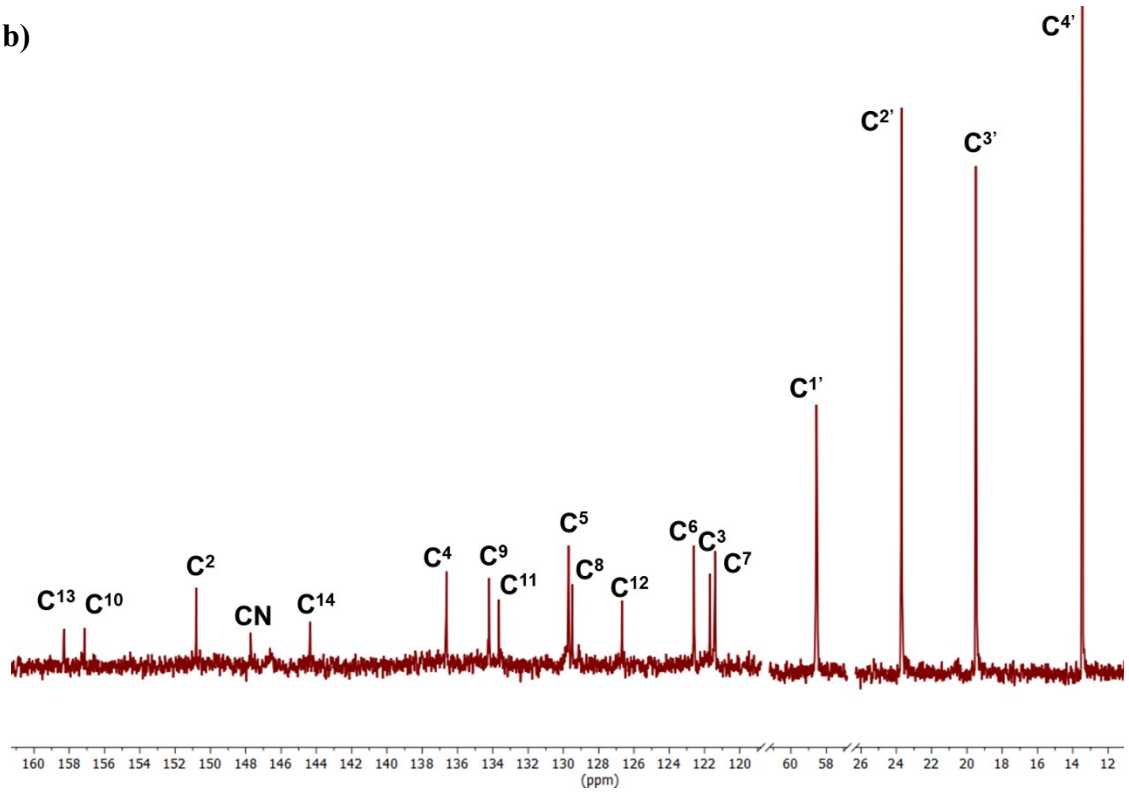

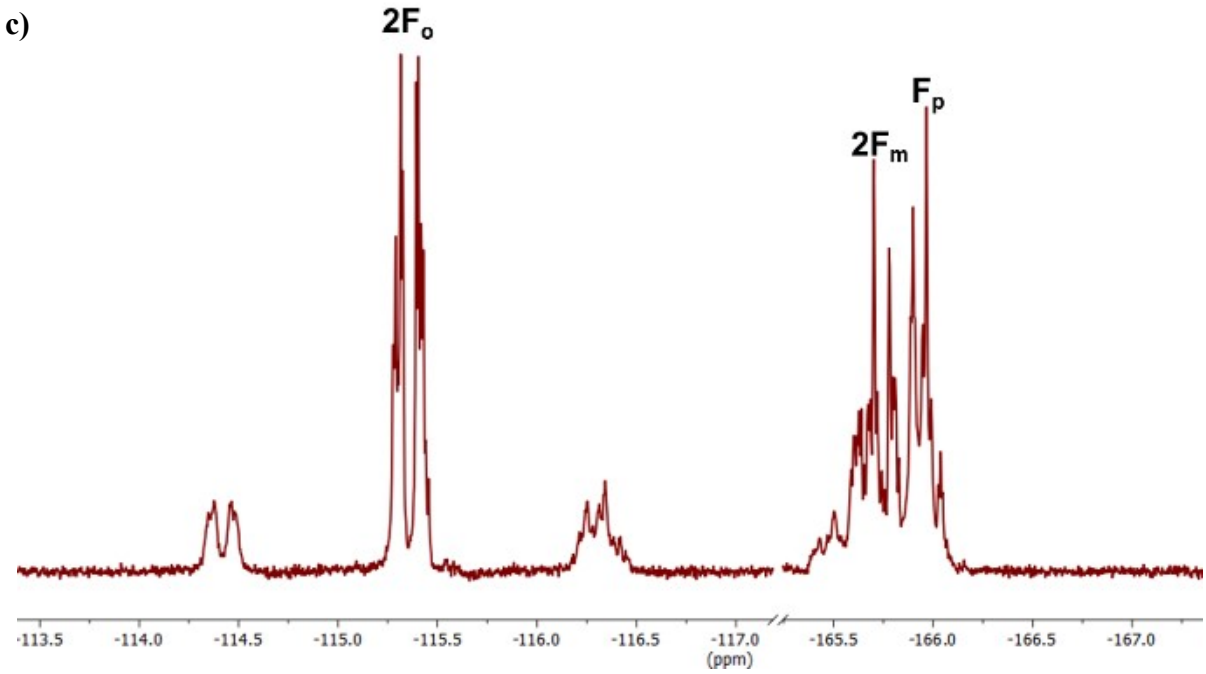

Figure S1. NMR spectra of **1** in $CDCl_3$ at 298 K, a) ^{1}H, b) $^{13}C\{^{1}H\}$, c) $^{19}F\{^{1}H\}$.

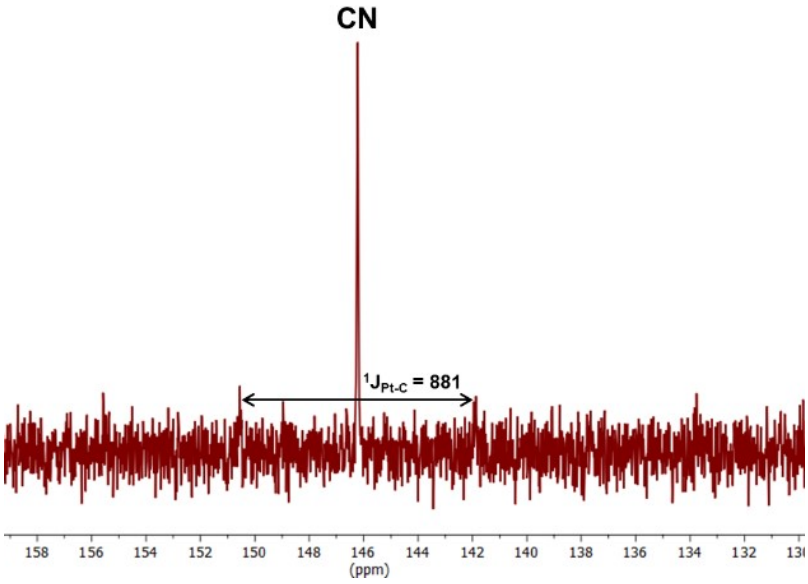

Figure S2. Selected region of the $^{13}C\{^{1}H\}$ NMR spectra of K[{Pt(bzq)(C_6F_5)(^{13}CN)}Tl] (**1'**) in $CDCl_3$.

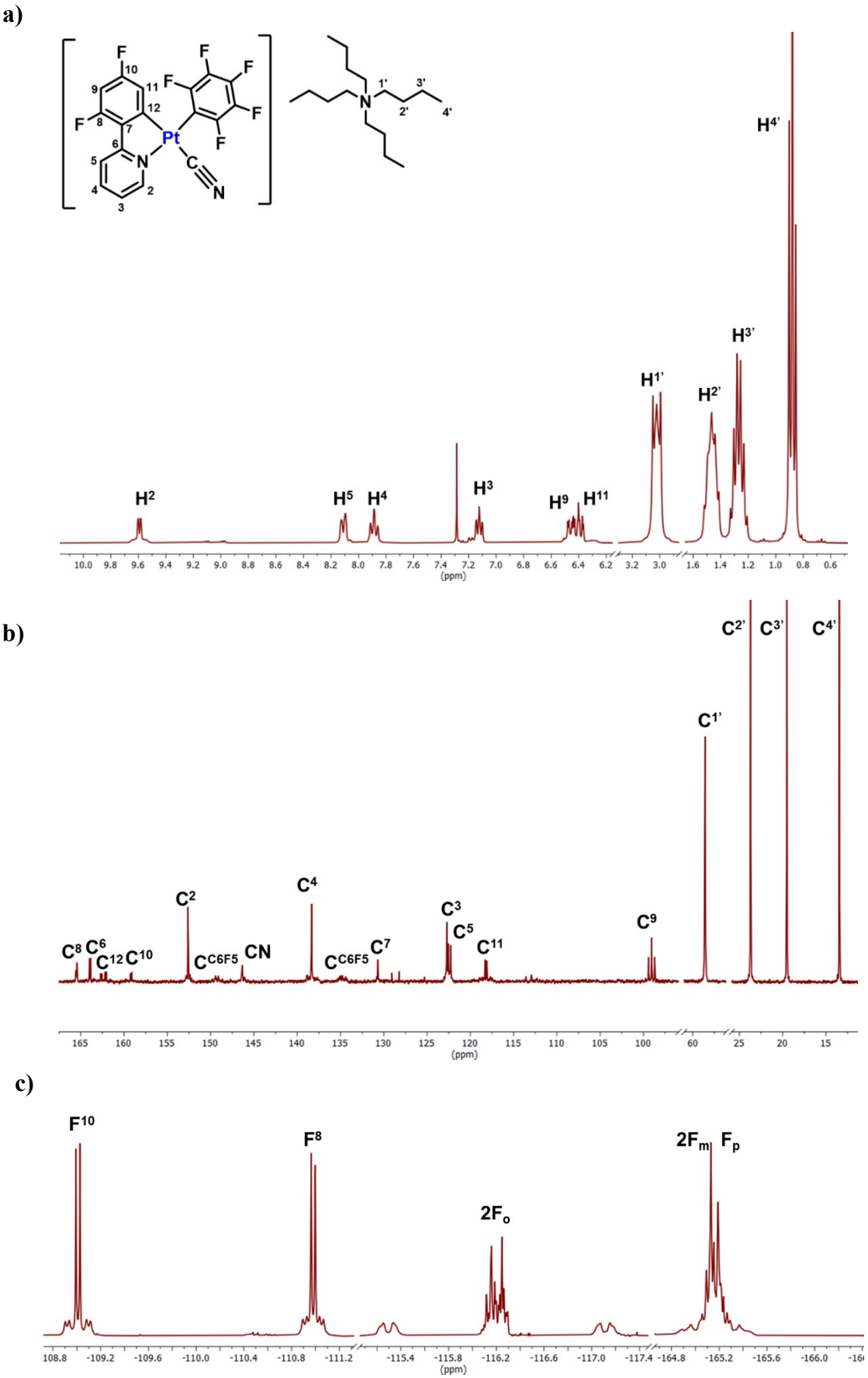

Figure S3. NMR spectra of **2** in $CDCl_3$ at 298 K, a) ^{1}H, b) $^{13}C\{^{1}H\}$, c) $^{19}F\{^{1}H\}$.

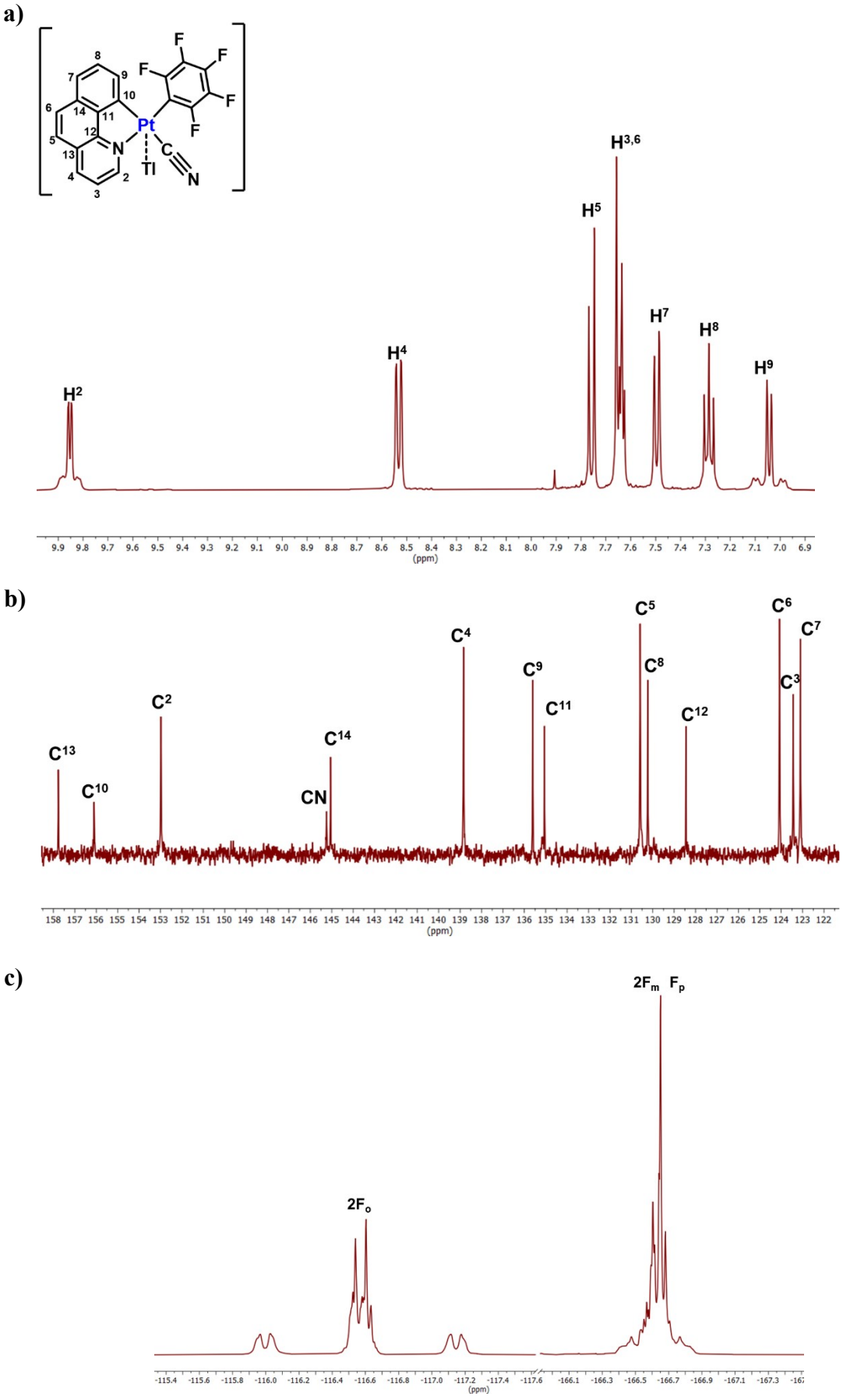

Figure S4. NMR spectra of **3** in THF-d_8 at 298 K, a) ^{1}H, b) $^{13}C\{^{1}H\}$, c) $^{19}F\{^{1}H\}$.

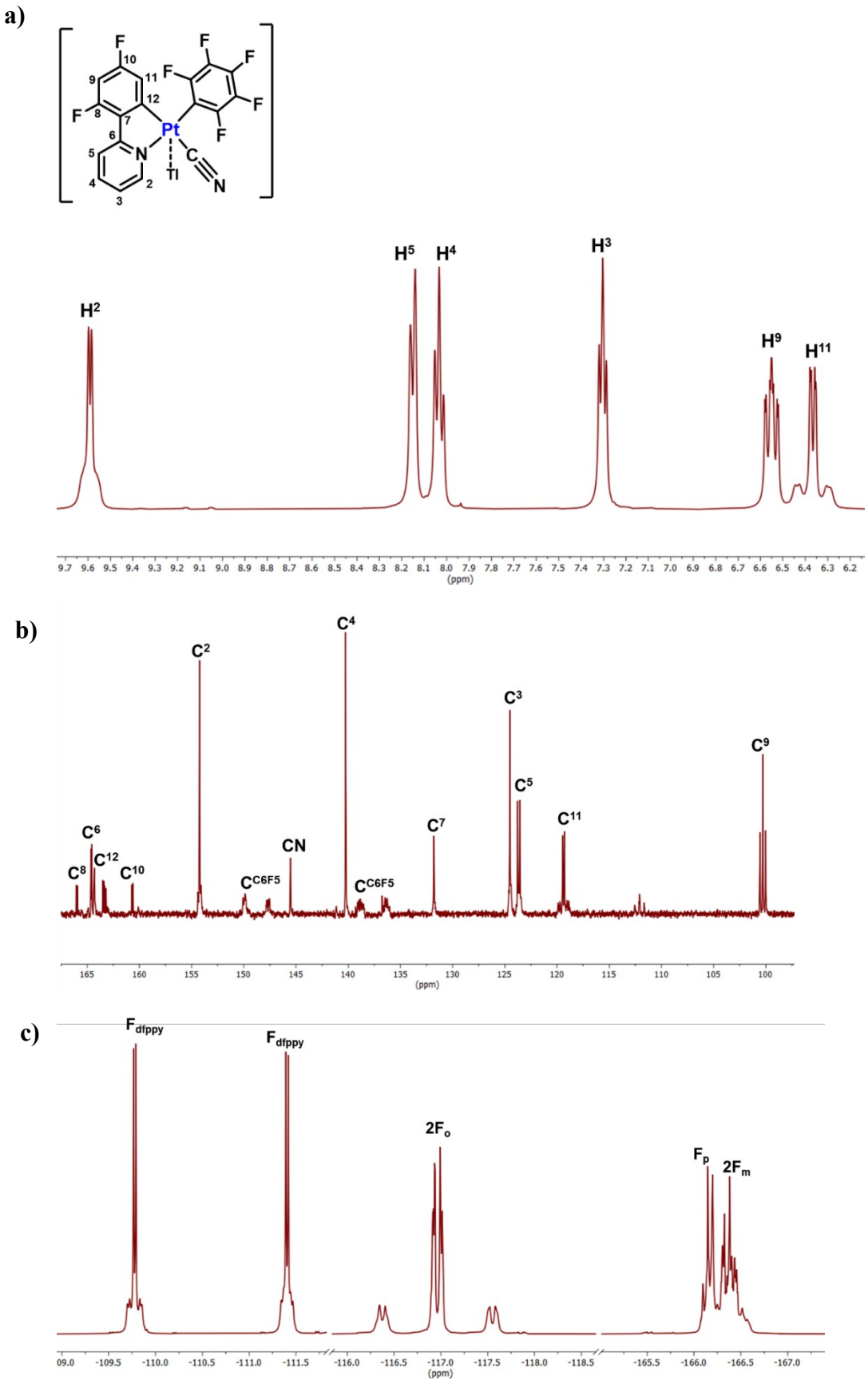

Figure S5. NMR spectra of **4** in THF-d_8 at 298 K, a) ^{1}H, b) $^{13}C\{^{1}H\}$, c) $^{19}F\{^{1}H\}$.

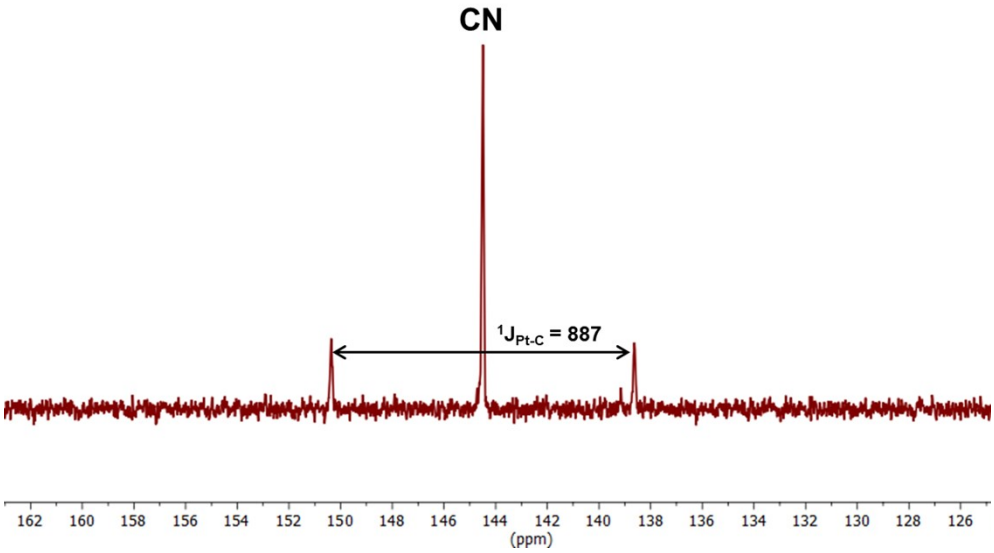

Figure S6. Selected region of the $^{13}C\{^{1}H\}$ NMR spectra of [{Pt(dfppy)(C_6F_5)(^{13}CN)}Tl] (**4'**) in THF-d_8

2.- Crystal Structures

Table S1. Crystal Data and Structure Refinement of $\{[Pt(bzq)(C_6F_5)(CN)Tl]\cdot THF\}_n$ $(\mathbf{3\cdot THF})_n$ and $[\{Pt(dfppy)(C_6F_5)(CN)\}Tl]_4\cdot C_4H_8O_2$ $\mathbf{[4]_4\cdot C_4H_8O_2}$

	$(\mathbf{3\cdot THF})_n$	$\mathbf{[4]_4\cdot C_4H_8O_2}$
Empirical formula	$\mathbf{C_{24}\ H_{16}F_5N_2OPtTl}$	$\mathbf{C_{76}H_{32}F_{28}N_8O_{1.22}\ Pt_4Tl_4}$
Molecular weight	842.85	3206.45
T (K)	293(2) K	100(2)
λ (Å)	0.71073	0.71076
Crystal system	Triclinic	Triclinic
Space group	P -1	P -1
Crystal size (mm)	0.241 × 0.058 × 0.034	0.275 × 0.067 × 0.050
a (Å)	11.887(2)	12.0740(8)
b (Å)	13.521(3)	12.6188(9)
c (Å)	14.790(3)	12.9418(9)
α (°)	74.76(3)	101.227(2)
β (°)	88.11(3)	101.332(3)
γ (°)	76.40(3)	98.078(3)
V (Å^3)	2228.1(9)	1863.3(2)
Z	4	1
ρ (calculated) (Mg/m^3)	2.513	2.858
μ (mm^{-1})	13.557	16.215
F (000)	1544	1442
θ range for data collection (°)	2.235 to 27.927	2.606 to 26.373
Index ranges	-15≤ h ≤ 15, -17 ≤ k ≤ 17, -19 ≤ l ≤ 19	-15 ≤ h ≤ 15, -15 ≤ k ≤ 15, -16 ≤ l ≤ 16
Reflections collected	126056	99409
Independent reflections	10673 [R(int) = 0.0341]	7619 [R(int) = 0.0517]
Data / restraints / parameters	10673 / 0 / 613	7619 / 0 / 550
Goodness-of-fit on F$^{2[a]}$	1.057	1.151
Final R indices [I>2σ(I)] [a]	R1 = 0.0150, wR2 = 0.0296	R1 = 0.0205, wR2 = 0.0461
R indices (all data) [a]	R1 = 0.0193, wR2 = 0.0311	R1 = 0.0227, wR2 = 0.0469
Largest diff. peak and hole (e Å^{-3}) (dmin/dmax)	1.445 and -0.956	2.179 and -1.138

[a] $R1 = \sum (|F_o| - |F_c|)/\sum|F_o|$; $wR_2 = [\sum w (F_o^2 - F_c^2)^2 / \sum w F_o^2]^{1/2}$; goodness of fit = $\{\sum [w (F_o^2 - F_c^2)^2]/(N_{obs} - N_{param})\}^{1/2}$; $w = [\sigma^2 (F_o) + (g1P)^2 + g2P]^{-1}$; $P = [\max(F_o^2;0 + 2F_c^2)/3$.

Table S2. Selected bond lengths (Å) and angles (°) of $\{[Pt(bzq)(C_6F_5)(CN)Tl]\cdot THF\}_n$ $(\mathbf{3\cdot THF})_n$ and $[\{Pt(dfppy)(C_6F_5)(CN)\}Tl]_4\cdot C_4H_8O_2$ $\mathbf{[4]_4\cdot C_4H_8O_2}$

$(\mathbf{3\cdot THF})_n$			
Distances (Å)		**Angles (°)**	
Pt(1)-C(1)	2.051(3)	C(1)-Pt(1)-N(1)	80.80(10)
Pt(1)-N(1)	2.097(2)	C(15)-Pt(1)-C(1)	93.78(11)
Pt(1)-C(15)	2.030(3)	C(14)-Pt(1)-C(1)	172.49(10)
Pt(1)-C(14)	2.024(3)	C(14)-Pt(1)-C(15)	91.75(11)
Pt(1)-Tl(1)	3.0279(7)	C(14)-Pt(1)-N(1)	93.71(10)
Pt(1)-Tl(2)	3.0402(7)	C(15)-Pt(1)-N(1)	174.54(9)
Tl(2)-O(1)	2.667(2)	C(14)-Pt(1)-Tl(1)	91.83(8)
Tl(2)-N(2)	2.723(2)	C(15)-Pt(1)-Tl(1)	104.64(8)
Tl(2)-Pt(2)	3.0140(7)	C(1)-Pt(1)-Tl(1)	81.85(8)
Pt(2)-C(35)	2.024(3)	N(1)-Pt(1)-Tl(1)	75.41(7)
Pt(2)-C(34)	2.027(3)	C(14)-Pt(1)-Tl(2)	91.87(8)
Pt(2)-C(21)	2.052(3)	C(15)-Pt(1)-Tl(2)	98.03(8)
Pt(2)-N(3)	2.097(2)	C(1)-Pt(1)-Tl(2)	92.39(8)
Pt(2)-Tl(1)#1	2.9795(6)	N(1)-Pt(1)-Tl(2)	81.60(6)
Tl(1)-N(4)	2.669(3)	Tl(1)-Pt(1)-Tl(2)	156.900(9)
		O(1)-Tl(2)-N(2)	99.56(7)
		O(1)-Tl(2)-Pt(2)	102.43(6)
		N(2)-Tl(2)-Pt(2)	93.90(6)
		O(1)-Tl(2)-Pt(1)	95.76(6)
		N(2)-Tl(2)-Pt(1)	97.27(6)
		Pt(2)-Tl(2)-Pt(1)	156.739(9)
		C(35)-Pt(2)-C(34)	89.84(11)
		C(35)-Pt(2)-C(21)	94.15(11)
		C(34)-Pt(2)-C(21)	174.93(10)
		C(35)-Pt(2)-N(3)	174.45(9)
		C(34)-Pt(2)-N(3)	94.83(10)
		C(21)-Pt(2)-N(3)	81.03(10)
		C(35)-Pt(2)-Tl(1)#1	94.19(8)
		C(34)-Pt(2)-Tl(1)#1	93.85(8)
		C(21)-Pt(2)-Tl(1)#1	82.76(8)
		N(3)-Pt(2)-Tl(1)#1	82.54(6)
		C(35)-Pt(2)-Tl(2)	98.67(8)
		C(34)-Pt(2)-Tl(2)	89.15(8)
		C(21)-Pt(2)-Tl(2)	93.33(8)
		N(3)-Pt(2)-Tl(2)	84.41(6)
$\mathbf{[4]_4\cdot C_4H_8O_2}$			
Distances (Å)		**Angles (°)**	
Pt(1)-C(1)#1	2.039(4)	C(1)#1-Pt(1)-N(1)#1	80.12(17)
Pt(1)-N(1)#1	2.082(4)	C(13)#1-Pt(1)-Tl(2)	99.42(12)
Pt(1)-C(12)#1	2.021(5)	C(12)#1-Pt(1)-Tl(2)	85.68(12)
Pt(1)-C(13)#1	2.016(4)	C(1)#1-Pt(1)-Tl(2)	95.98(11)
Pt(1)-Tl(2)	3.0518(3)	N(1)#1-Pt(1)-Tl(2)	80.65(10)
Pt(1)-Tl(1)#1	3.0736(3)	C(13)#1-Pt(1)-Tl(1)#1	97.85(12)
Tl(2)-N(2)	2.626(4)	C(12)#1-Pt(1)-Tl(1)#1	95.24(12)
Tl(1)-N(4)	2.596(4)	C(1)#1-Pt(1)-Tl(1)#1	82.33(11)
Pt(2)-C(31)	2.014(4)	N(1)#1-Pt(1)-Tl(1)#1	82.13(10)
Pt(2)-C(30)	2.007(4)	Tl(2)-Pt(1)-Tl(1)#1	162.723(8)
Pt(2)-C(19)	2.025(4)	C(13)#1-Pt(1)-C(12)#1	88.74(17)
Pt(2)-N(3)	2.075(4)	C(13)#1-Pt(1)-C(1)#1	93.80(18)
Pt(2)-Tl(2)	2.9258(3)	C(12)#1-Pt(1)-C(1)#1	176.69(17)

	C(13)#1-Pt(1)-N(1)#1	173.88(16)
	C(12)#1-Pt(1)-N(1)#1	97.36(16)
	C(30)-Pt(2)-C(31)	88.76(17)
	C(30)-Pt(2)-C(19)	176.13(17)
	C(31)-Pt(2)-C(19)	94.46(17)
	C(30)-Pt(2)-N(3)	96.41(16)
	C(31)-Pt(2)-N(3)	174.50(15)
	C(19)-Pt(2)-N(3)	80.31(16)
	C(30)-Pt(2)-Tl(2)	97.04(12)
	C(31)-Pt(2)-Tl(2)	93.70(12)
	C(19)-Pt(2)-Tl(2)	84.93(11)
	N(3)-Pt(2)-Tl(2)	87.57(10)
	N(2)-Tl(2)-Pt(2)	91.43(9)
	N(2)-Tl(2)-Pt(1)	97.96(9)
	Pt(2)-Tl(2)-Pt(1)	160.299(8)
	N(4)-Tl(1)-Pt(1)#1	89.06(9)

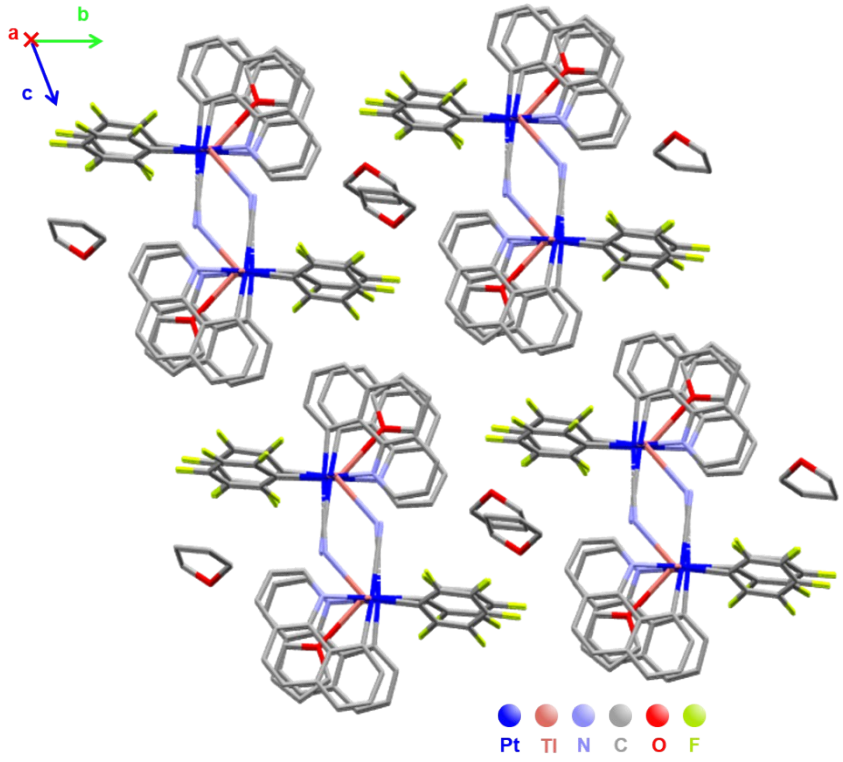

Figure S7. Packing of the crystal structure of (**3**·**THF**)$_n$.

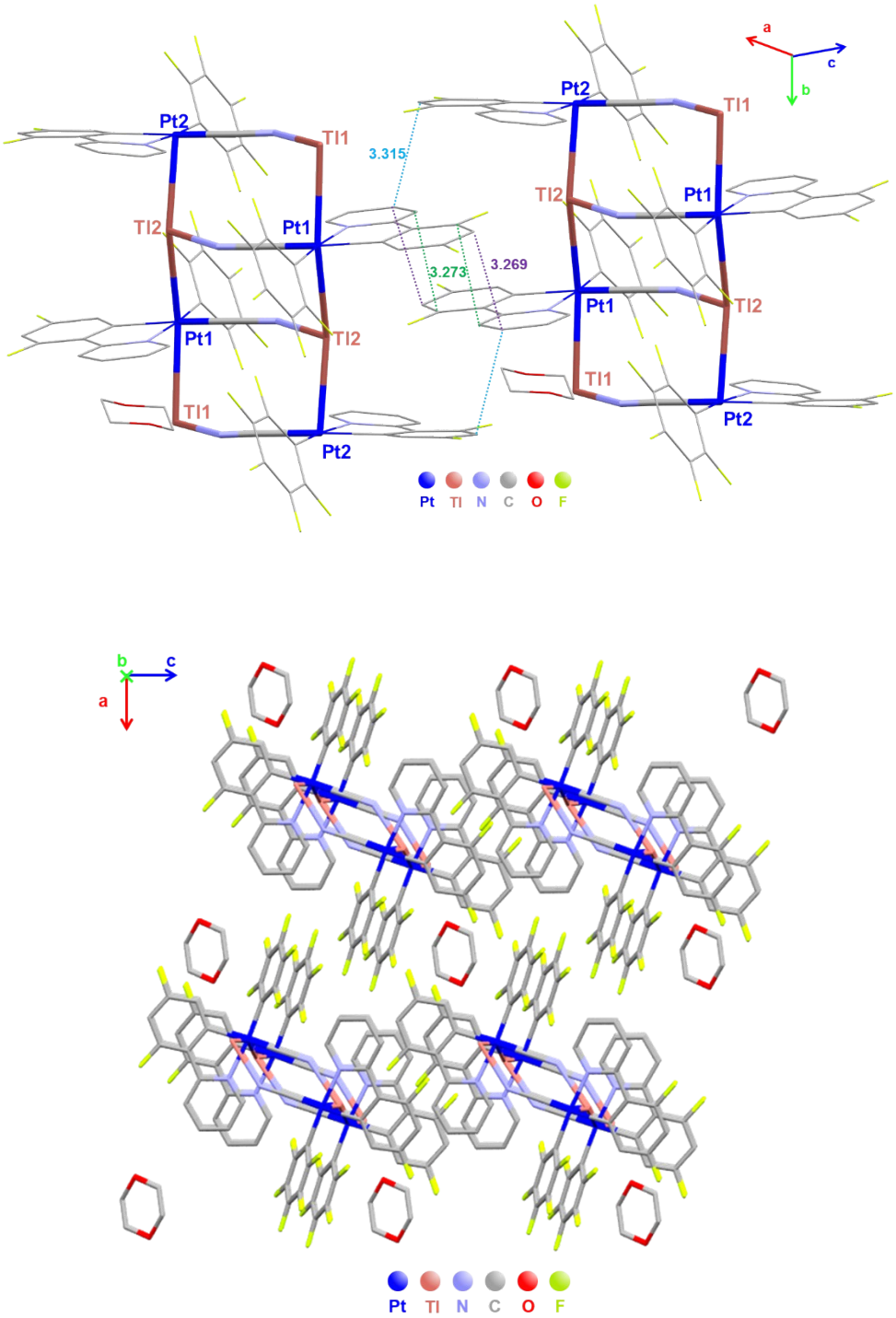

Figure S8. Two different views of the packing of the crystal structure of $[\mathbf{4}]_4 \cdot C_4H_8O_2$.

3. Photophysical Properties and Theoretical Calculations

Table S3. Absorption data for complexes **1**–**4** in THF (5×10^{-5} M) and solid state at 298 K

Compound	Media	λ_{abs}/nm (ε x 10^{-3} M^{-1} cm^{-1})
1	**THF**	221(35.7), 254(34.9), 309(10.0), 341(7.0), 351(5.4), 378(3.4), 430(1.5), with tail to 450
	Solid	286, 309, 328, 347, 375, 393, 415, 427, 461_{sh}, with tail to 500
2	**THF**	219(25.2), 256(29.6), 319(7.2),353(4.6), 382(2.5), with tail to 415
	Solid	284, 312, 322, 350, 372, 390, 426_{sh}, 456, 464, 471, with tail to 475
3	**THF**	222(34.0), 235(31.0), 248(32.0), 303(11.5), 340(6.2), 371(2.7), 420(1.4), with tail to 440
	Solid	296, 310, 370, 422, 437, 492, 519, with tail to 575
3-MeOH	**Solid**	295, 311, 334, 358, 375, 399, 420, 431, 465, 499, with tail to 575
3-CH_2Cl_2	**Solid**	287, 308, 338, 364, 391, 416, 468, 492, 527, 555, with tail to 620
3-THF	**Solid**	306, 325, 350, 360, 370, 375, 397, 411, 445, 475, 495, 514, 528, 580, with tail to 675
3-Et_2O	**Solid**	294, 310, 330, 342, 357, 394, 421, 447, 474, 505, with tail to 575
3-ground	**Solid**	290, 310, 328, 346, 379, 398, 415, 467, 496, 516, 560, with tail to 640
4	**THF**	222(24.1), 255(27.0), 318(7.2), 346(4.3), 374(2.3), with tail to 400
	Solid	288, 308, 334, 365, 387, 410, 425, 458, with tail to 525
4-MeOH	**Solid**	295, 328, 344, 362, 387, 417, 428, 460, 492, 520, with tail to 573
4-ground	**Solid**	280, 290, 308, 320, 359, 376, 388, 465, with tail to 550

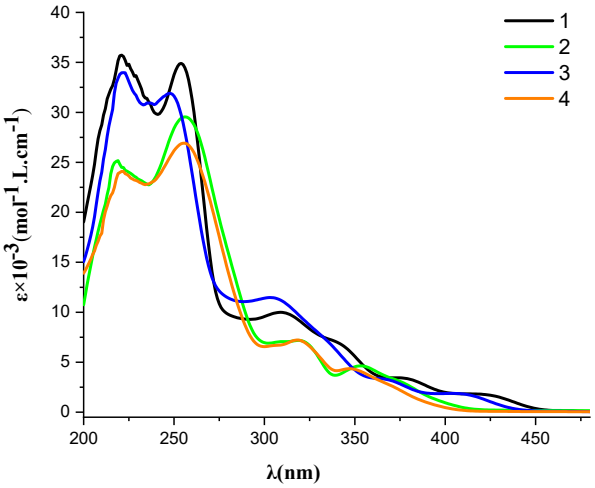

Figure S9. UV-Vis absorption spectra of complexes **1-4** in THF 5×10^{-5} M at 298 K.

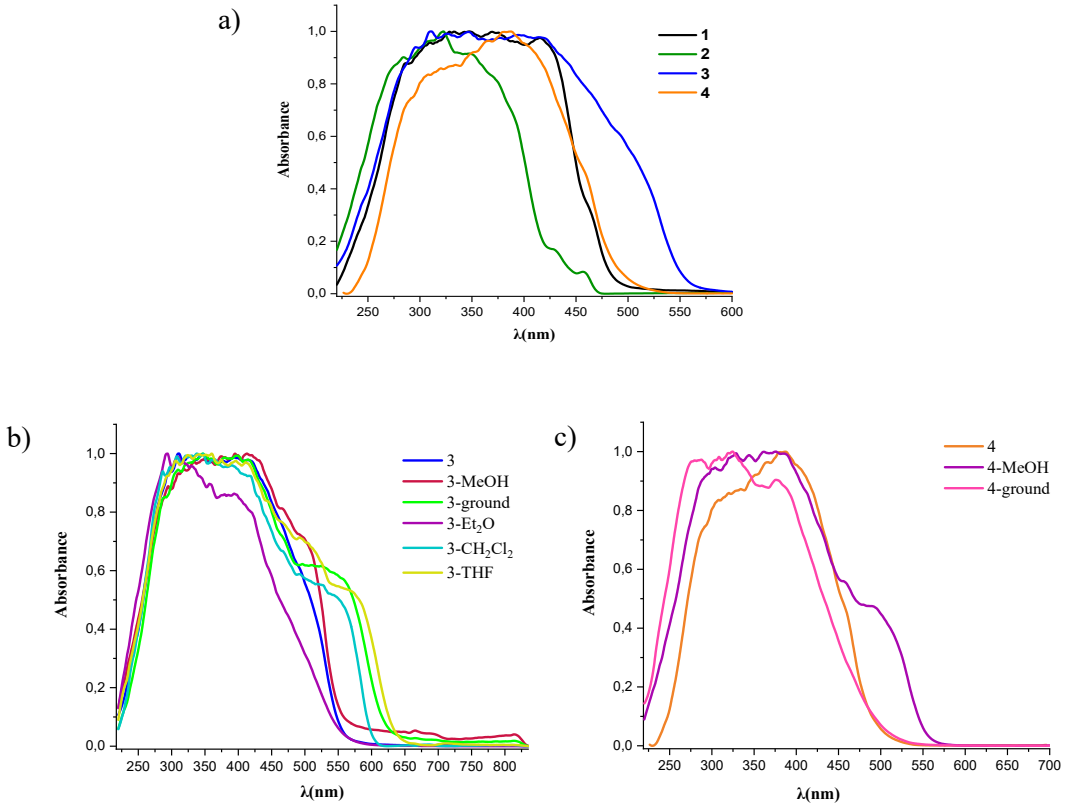

Figure S10. Absorption spectra in solid state of the complexes a) **1–4**, b) **3**, c) **4**.

Table S4. Selected vertical excitation energies singlets (S_n) and first triplets computed by TDDFT (**THF**) with the orbitals involved for $\mathbf{1^-}$ and $\mathbf{2^-}$

[Pt(bzq)(C_6F_5)(CN)]$^-$ ($\mathbf{1^-}$)			
State	**λ/nm**	***f***	**Transition (% Contribution)**
T_1	467.46	0.0	H-3→LUMO (27%), HOMO→LUMO (22%), HOMO→L+1 (30%)
T_2	443.02	0.0	HOMO→LUMO (71%), HOMO→L+1 (16%)
T_3	389.69	0.0	H-3→LUMO (52%), HOMO→L+1 (36%)
S_1	399.33	0.0436	HOMO→LUMO (95%)
S_2	374.54	0.0028	H-2→LUMO (21%), H-1→LUMO (78%)
S_3	352.70	0.0	H-2→LUMO (77%), H-1→LUMO (20%)
S_4	337.60	0.0347	H-3→LUMO (26%), HOMO→L+1 (67%)
S_5	317.57	0.2178	H-3→LUMO (61%), HOMO→L+1 (27%)
S_6	316.62	0.0056	H-2→L+1 (17%), H-1→L+1 (81%)
S_7	305.42	0.0169	H-5→LUMO (79%), H-4→LUMO (13%)
S_8	304.19	0.0	H-2→L+1 (80%), H-1→L+1 (17%)
S_9	301.01	0.0321	H-6→LUMO (40%), H-3→L+1 (43%)
S_{10}	298.24	0.0002	H-5→LUMO (13%), H-4→LUMO (85%)
S_{11}	282.97	0.0001	H-7→LUMO (95%)
S_{12}	278.75	0.1262	H-6→LUMO (41%), H-5→L+1 (12%), H-3→L+1 (34%)
[Pt(dfppy)(C_6F_5)(CN)]$^-$ ($\mathbf{2^-}$)			
State	**λ/nm**	***f***	**Transition (% Contribution)**
T_1	434.70	0.0	H-3→LUMO (20%), HOMO→LUMO (64%)
T_2	373.98	0.0	H-2→LUMO (41%), H-1→LUMO (56%)
T_3	366.19	0.0	H-3→LUMO (50%), HOMO→LUMO (30%)
S_1	364.95	0.0338	HOMO→LUMO (97%)
S_2	358.52	0.0061	H-2→LUMO (40%), H-1→LUMO (60%)
S_3	339.47	0.0001	H-2→LUMO (59%), H-1→LUMO (39%)
S_4	309.60	0.1026	H-5→LUMO (25%), H-3→LUMO (66%)
S_5	302.02	0.0491	H-5→LUMO (35%), H-3→LUMO (15%), HOMO→L+1 (46%)
S_6	292.62	0.0009	H-4→LUMO (94%)
S_7	290.02	0.0	H-2→L+1 (41%), H-1→L+1 (58%)
S_8	288.87	0.2186	H-5→LUMO (30%), HOMO→L+1 (50%)
S_9	277.28	0.0001	H-2→L+1 (57%), H-1→L+1 (39%)
S_{10}	267.78	0.0001	H-8→LUMO (12%), H-6→LUMO (84%)
S_{11}	261.05	0.0989	H-7→LUMO (10%), H-5→L+1 (18%), H-3→L+1 (42%)
S_{12}	255.74	0.0682	H-7→LUMO (10%), H-2→L+3 (45%), H-1→L+3 (24%)

Table S5. Composition (%) of Frontier MOs in terms of ligands and metals in the ground

state in **THF** for $\mathbf{1^-}$ and $\mathbf{2^-}$					
$[Pt(bzq)(C_6F_5)(CN)]^-$ ($\mathbf{1^-}$)					
MO	**eV**	**Pt**	**bzq**	**CN^-**	**C_6F_5**
LUMO+5	0.63	3	1	0	96
LUMO+4	0.62	1	2	0	97
LUMO+3	0.51	40	10	3	46
LUMO+2	0.14	8	87	2	2
LUMO+1	-0.82	5	94	1	0
LUMO	-1.39	3	96	0	0
HOMO	-5.17	30	63	6	0
HOMO-1	-5.50	71	7	1	21
HOMO-2	-5.54	50	1	5	43
HOMO-3	-5.84	40	55	1	4
HOMO-4	-5.97	2	1	0	97
HOMO-5	-6.21	55	38	5	2
$[Pt(dfppy)(C_6F_5)(CN)]^-$ ($\mathbf{2^-}$)					
MO	**eV**	**Pt**	**dfppy**	**CN^-**	**C_6F_5**
LUMO+5	0.58	5	1	1	94
LUMO+4	0.58	1	3	0	96
LUMO+3	0.44	38	13	3	46
LUMO+2	0.16	20	72	5	3
LUMO+1	-0.57	1	99	0	0
LUMO	-1.29	7	92	1	1
HOMO	-5.46	41	50	9	0
HOMO-1	-5.61	58	7	2	34
HOMO-2	-5.64	63	0	3	33
HOMO-3	-5.95	19	73	2	6
HOMO-4	-6.01	2	4	0	94
HOMO-5	-6.15	69	28	0	3

a)

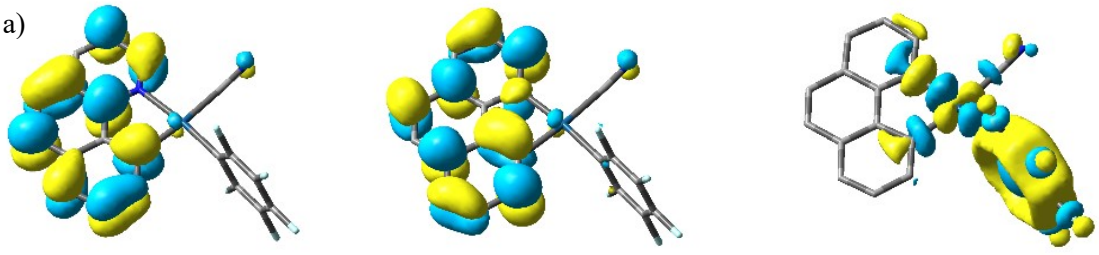

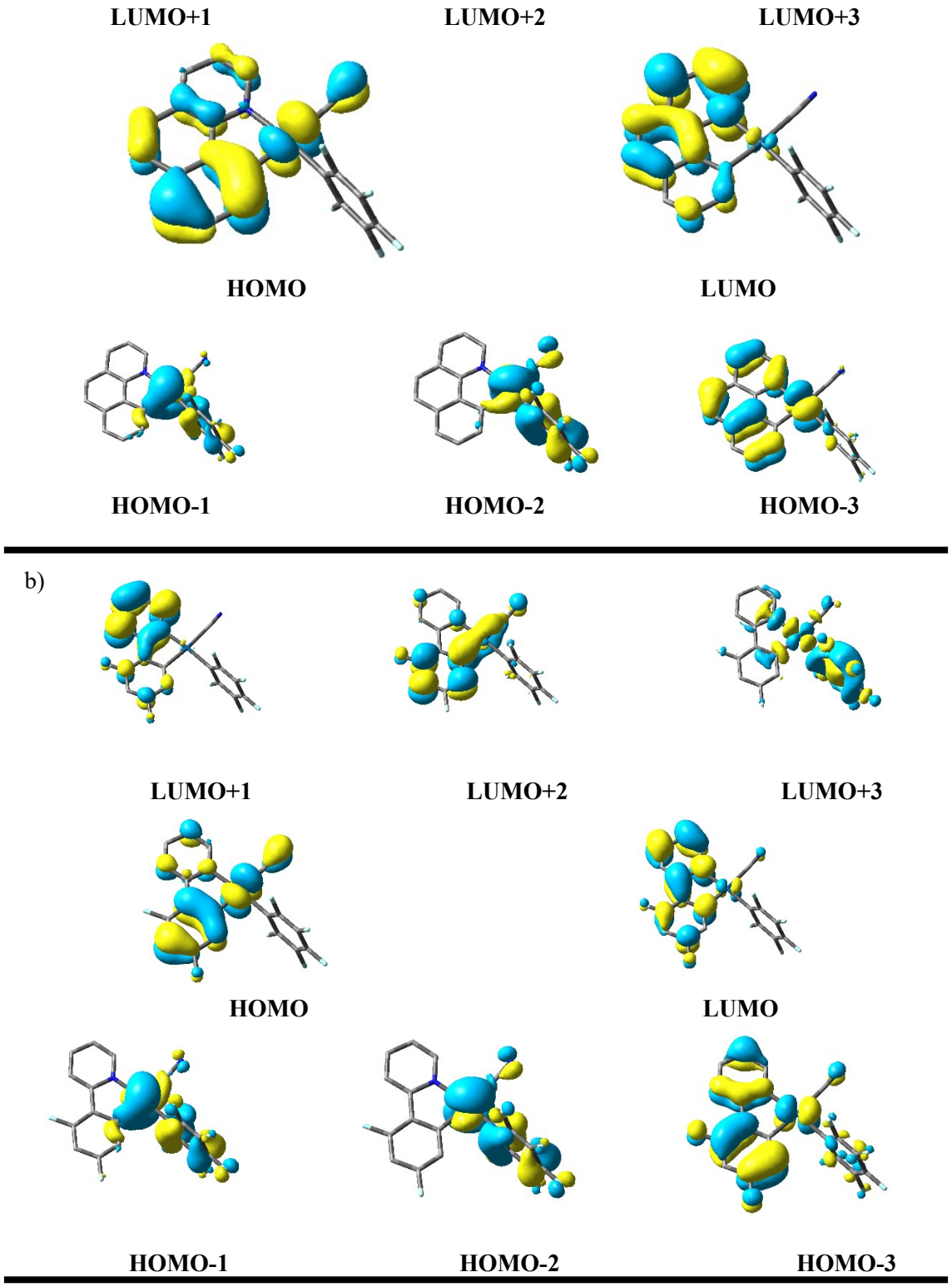

Figure S11. Selected frontier molecular orbitals for a) $\mathbf{1}^{-}$ and b) $\mathbf{2}^{-}$ in the ground state in **THF**.

$[Pt(bzq)(C_6F_5)(CN)]^{-}$ (1^{-})	
SOMO	**SOMO-1**

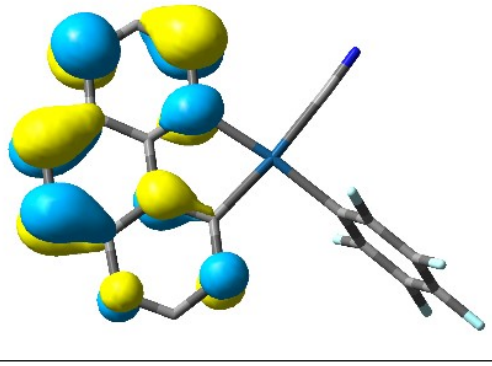	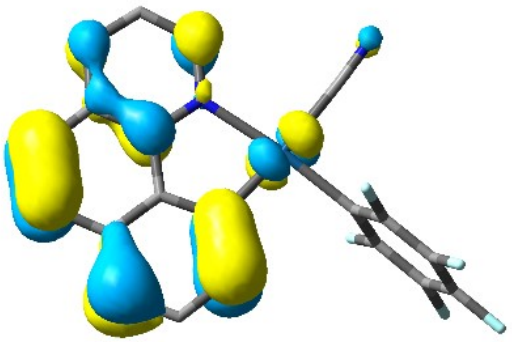
-2.88eV	-3.83eV
Pt 1%, bzq 99%, CN^- 0%, C_6F_5 0%	Pt 8%, bzq 90%, CN^- 2%, C_6F_5 0%
$[Pt(dfppy)(C_6F_5)(CN)]^-$ (2^-)	
SOMO	**SOMO-1**
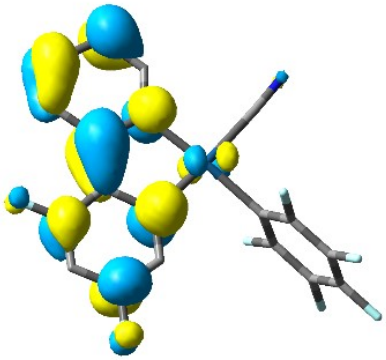	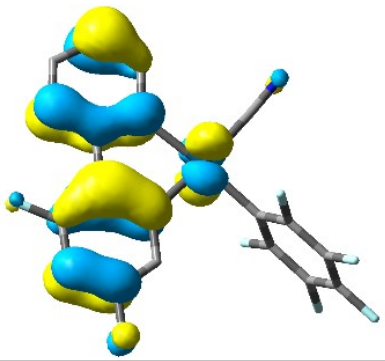
-2.95eV	-4.01eV
Pt 6%, dfppy 93%, CN^- 1%, C_6F_5 0%	Pt 13%, dfppy 85%, CN^- 1%, C_6F_5 0%

$[Pt(bzq)(C_6F_5)(CN)]^-$	**$[Pt(dfppy)(C_6F_5)(CN)]^-$**
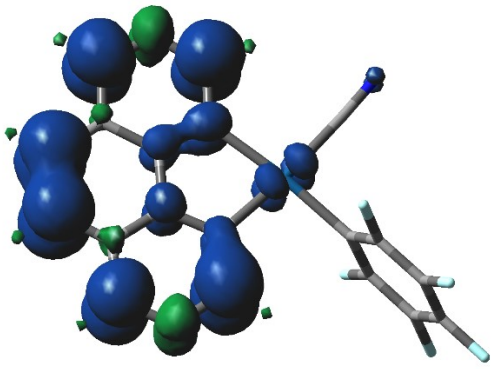	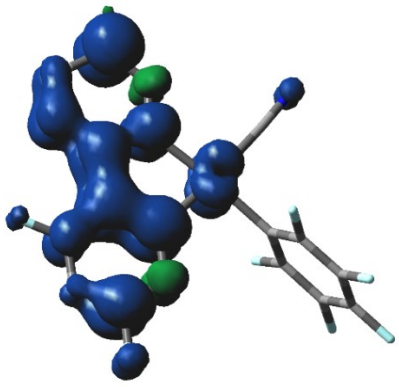
Spin density on Pt 0.069	**Spin density on Pt 0.187**

Figure S12. Plots and composition (%) of frontier MOs of the first triplet state and spin distribution for the lowest triplet excited state in the mononuclear $\mathbf{1}^-$ and $\mathbf{2}^-$ in **THF**.

Table S6. Selected vertical excitation energies singlets (S_n) and first triplets computed by TD-DFT with the orbitals involved for **3·(THF)$_3$** and **4·(THF)$_3$**.

[Pt(bzq)(C$_6$F$_5$)(CN)Tl(THF)$_3$] 3·(THF)$_3$			
State	**λ/nm**	***f***	**Transition (% Contribution)**
T_1	464.984011	0.0	H-3→LUMO (26%), HOMO→LUMO (19%), HOMO→L+1 (36%)
T_2	437.42357	0.0	HOMO→LUMO (74%), HOMO→L+1 (15%)
T_3	384.563699	0.0	H-3→LUMO (43%), HOMO→L+1 (34%)
S_1	389.321537	0.0501	HOMO→LUMO (95%)
S_2	362.66223	0.0206	H-1→LUMO (97%)
S_3	344.063651	0.0122	H-2→LUMO (95%)
S_4	329.883292	0.0316	H-3→LUMO (36%), HOMO→L+1 (58%)
S_5	311.484616	0.1623	H-3→LUMO (47%), H-1→L+1 (13%), HOMO→L+1 (31%)
S_6	306.821096	0.0462	H-1→L+1 (85%)
S_7	299.766288	0.0137	H-5→LUMO (13%), H-3→L+1 (12%), H-2→L+1 (64%)
S_8	298.776626	0.0057	H-4→LUMO (94%)
S_9	294.94561	0.0207	H-5→LUMO (21%), H-3→L+1 (33%), H-2→L+1 (30%)
S_{10}	291.910947	0.0517	H-6→LUMO (79%), H-5→LUMO (10%)
S_{11}	278.821006	0.0253	H-5→LUMO (30%), HOMO→L+2 (47%)
S_{12}	277.417293	0.0047	H-10→LUMO (23%), H-9→LUMO (26%), H-8→LUMO (33%)
[Pt(dfppy)(C$_6$F$_5$)(CN)Tl(THF)$_3$] 4·(THF)$_3$			
State	**λ/nm**	***f***	**Transition (% Contribution)**
T_1	432.479896	0.0	H-3→LUMO (14%), HOMO→LUMO (68%)
T_2	364.667598	0.0	H-2→LUMO (39%), H-1→LUMO (54%)
T_3	358.25051	0.0	H-3→LUMO (50%), HOMO→LUMO (24%)
S_1	354.704287	0.0428	HOMO→LUMO (96%)
S_2	343.463174	0.0386	H-2→LUMO (39%), H-1→LUMO (60%)
S_3	333.36023	0.01	H-2→LUMO (59%), H-1→LUMO (38%)
S_4	307.208823	0.1163	H-3→LUMO (86%)
S_5	292.931687	0.0308	H-5→LUMO (52%), H-4→LUMO (25%), HOMO→L+1 (18%)
S_6	292.434221	0.0095	H-5→LUMO (17%), H-4→LUMO (74%)
S_7	279.973211	0.1422	H-5→LUMO (14%), H-1→L+1 (18%), HOMO→L+1 (48%)
S_8	278.758317	0.0549	H-2→L+1 (35%), H-1→L+1 (39%), HOMO→L+1 (15%)
S_9	271.452767	0.0008	H-7→LUMO (77%), H-6→LUMO (11%)
S_{10}	269.933894	0.0138	H-2→L+1 (49%), H-1→L+1 (35%)
S_{11}	266.504743	0.0056	H-9→LUMO (27%), H-7→LUMO (10%), H-6→LUMO (51%)
S_{12}	264.24411	0.1127	HOMO→L+2 (68%)

Table S7. Composition (%) of Frontier MOs in terms of ligands and metals in the ground state for **3·(THF)$_3$** and **4·(THF)$_3$**.

[Pt(bzq)(C$_6$F$_5$)(CN)Tl(THF)$_3$] 3·(THF)$_3$							
MO	**eV**	**Pt**	**Tl**	**bzq**	**CN$^-$**	**C$_6$F$_5$**	**THF**
LUMO+5	0.14	4	11	6	0	78	2
LUMO+4	-0.13	13	28	40	1	15	4
LUMO+3	-0.28	22	42	15	1	14	5
LUMO+2	-0.54	9	42	41	3	2	3
LUMO+1	-1.27	5	5	87	2	0	0
LUMO	-1.83	4	2	93	0	1	0
HOMO	-5.68	21	1	73	4	0	1
HOMO-1	-5.98	65	17	4	1	6	7
HOMO-2	-6.05	26	1	6	6	62	0
HOMO-3	-6.36	16	0	77	1	6	0
HOMO-4	-6.43	1	0	3	0	95	0
HOMO-5	-6.81	32	0	53	12	0	2
[Pt(dfppy)(C$_6$F$_5$)(CN)Tl(THF)$_3$] 4·(THF)$_3$							
MO	**eV**	**Pt**	**Tl**	**dfppy**	**CN$^-$**	**C$_6$F$_5$**	**THF**
LUMO+5	0.08	2	1	4	0	92	0
LUMO+4	-0.01	6	14	26	1	52	1
LUMO+3	-0.36	25	32	13	2	24	4
LUMO+2	-0.65	11	47	35	4	2	1
LUMO+1	-1.01	1	3	96	0	0	0
LUMO	-1.79	8	5	85	1	1	0
HOMO	-6.04	30	1	63	6	0	0
HOMO-1	-6.17	46	8	7	1	35	2
HOMO-2	-6.18	47	10	1	4	36	2
HOMO-3	-6.43	11	0	83	3	2	1
HOMO-4	-6.52	1	0	1	0	97	0
HOMO-5	-6.86	75	0	18	1	3	3

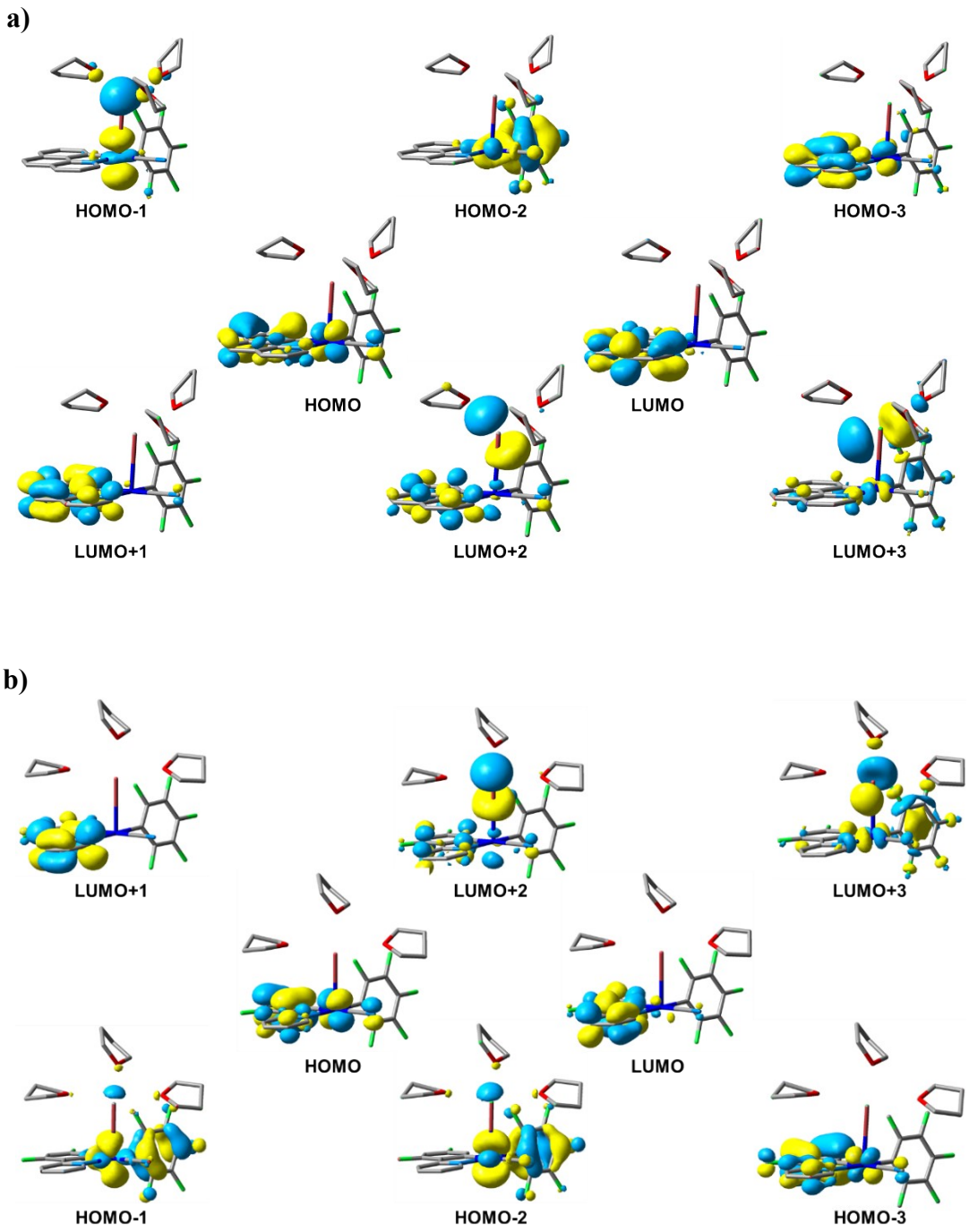

Figure S13. Selected frontier molecular orbitals for the models a) **3**·**(THF)$_3$** and b) **4**·**(THF)$_3$** in the ground state.

Table S8. Selected vertical excitation energies singlets (S_n) and first triplets computed by TDDFT (**Solid State**) with the orbitals involved for $\mathbf{1}^-$, $\mathbf{2}^-$, **3** and **4**.

$[Pt(bzq)(C_6F_5)(CN)]^-$ ($\mathbf{1}^-$)			
State	**λ/nm**	***f***	**Transition (% Contribution)**
T_1	506.66	-	HOMO→LUMO (87%)
T_2	474.62	-	H-3→LUMO (24%), HOMO→L+1 (37%)
T_3	463.63	-	H-1→LUMO (95%)
S_1	456.60	0.0144	HOMO→LUMO (96%)
S_2	452.78	0.0009	H-1→LUMO (98%)
S_3	418.34	0.0	H-2→LUMO (97%)
S_4	375.33	0.0163	H-3→LUMO (20%), HOMO→L+1 (73%)
S_5	367.07	0.0019	H-1→L+1 (98%)
S_6	348.64	0.1402	H-3→LUMO (58%), HOMO→L+1 (23%)
S_7	347.49	0.0	H-2→L+1 (97%)
S_8	336.85	0.0034	H-4→LUMO (85%), H-3→LUMO (13%)
S_9	326.40	0.0225	H-5→LUMO (60%), H-3→L+1 (28%)
S_{10}	323.58	0.0	H-6→LUMO (92%)
S_{11}	314.45	0.0186	H-7→LUMO (19%), H-5→LUMO (24%), H-3→L+1 (43%)
S_{12}	301.05	0.0524	H-7→LUMO (62%), H-5→L+1 (11%), H-3→L+1 (13%)
$[Pt(dfppy)(C_6F_5)(CN)]^-$ ($\mathbf{2}^-$)			
State	**λ/nm**	***f***	**Transition (% Contribution)**
T_1	458.17	-	HOMO→LUMO (77%)
T_2	431.88	-	H-1→LUMO (94%)
T_3	399.85	-	H-4→LUMO (59%), HOMO→LUMO (18%)
S_1	415.27	0.0022	H-1→LUMO (97%)
S_2	409.74	0.0138	HOMO→LUMO (96%)
S_3	386.68	0.0	H-2→LUMO (95%)
S_4	337.51	0.0253	H-4→LUMO (56%), HOMO→L+1 (38%)
S_5	333.77	0.0	H-1→L+1 (95%)
S_6	329.89	0.0645	H-4→LUMO (35%), HOMO→L+1 (59%)
S_7	320.14	0.0002	H-3→LUMO (99%)
S_8	316.04	0.0	H-2→L+1 (93%)
S_9	302.06	0.068	H-5→LUMO (62%), H-4→L+1 (31%)
S_{10}	300.63	0.0	H-6→LUMO (88%)
S_{11}	279.61	0.1476	H-5→LUMO (21%), H-4→L+1 (53%)
S_{12}	279.60	0.0047	H-7→LUMO (86%)
3 (optimized model Pt_4Tl_4 based on the reported crystallographic structure)			
State	**λ/nm**	***f***	**Transition (% Contribution)**
T_1	537.24	-	HOMO→LUMO (90%)
T_2	488.15	-	H-1→L+1 (75%)
T_3	472.83	-	H-13→L+2 (12%), H-3→L+2 (40%), H-3→L+7 (15%)
S_1	443.43	0.0791	H-1→LUMO (24%), HOMO→LUMO (66%)
S_2	439.78	0.0008	H-1→LUMO (56%), HOMO→LUMO (32%)
S_3	431.18	0.1502	H-1→LUMO (11%), H-1→L+1 (12%), HOMO→L+1 (69%)
S_4	422.88	0.0835	H-3→LUMO (27%), H-2→LUMO (52%)
S_5	418.81	0.0023	H-1→L+2 (16%), HOMO→L+2 (71%)
S_6	414.94	0.0248	H-3→LUMO (32%), H-2→LUMO (19%), H-2→L+1 (15%)
S_7	412.03	0.005	H-3→LUMO (14%), H-1→L+1 (59%), HOMO→L+1 (13%)

S_8	408.04	0.0091	H-3→LUMO (13%), H-3→L+1 (31%), H-2→LUMO (19%), H-2→L+1 (16%)
S_9	403.63	0.0018	H-5→LUMO (10%), H-4→LUMO (79%)
S_{10}	401.99	0.0029	H-5→LUMO (62%), H-4→LUMO (15%)
S_{11}	398.69	0.0015	H-3→L+1 (36%), H-2→L+1 (46%)
S_{12}	395.96	0.0168	H-3→L+1 (11%), H-3→L+2 (14%), H-2→L+2 (11%), H-1→L+3 (21%), HOMO→L+3 (11%)
4 (optimized model Pt_4Tl_4)			
State	**λ/nm**	***f***	**Transition (% Contribution)**
T_1	439.30	-	H-1→L+2 (19%), HOMO→LUMO (11%), HOMO→L+3 (16%)
T_2	439.29	-	H-1→L+3 (11%), HOMO→L+2 (15%)
T_3	438.65	-	H-11→L+1 (32%), H-10→LUMO (33%)
S_1	383.64	0.0018	H-2→LUMO (19%), H-1→LUMO (59%)
S_2	383.54	0.2258	HOMO→LUMO (89%)
S_3	378.34	0.0	H-2→LUMO (70%), H-1→LUMO (20%)
S_4	375.37	0.0643	H-3→LUMO (93%)
S_5	366.52	0.0	H-4→LUMO (27%), H-1→LUMO (12%), HOMO→L+1 (42%)
S_6	365.08	0.1146	H-5→LUMO (20%), H-2→L+1 (22%), H-1→L+1 (37%)
S_7	364.05	0.0	H-4→LUMO (56%), HOMO→L+1 (37%)
S_8	361.82	0.0301	H-5→LUMO (61%), H-1→L+1 (33%)
S_9	358.91	0.019	H-10→LUMO (15%), H-2→L+1 (59%)
S_{10}	357.86	0.0	H-11→LUMO (17%), H-3→L+1 (59%)
S_{11}	355.72	0.0	H-11→LUMO (34%), H-10→L+1 (18%), H-3→L+1 (31%)
S_{12}	354.94	0.0336	H-11→L+1 (16%), H-10→LUMO (38%), H-2→L+1 (15%), H-1→L+1 (14%)

Table S9. Composition (%) of Frontier MOs in terms of ligands and metals in the ground state in **solid state** for **1^-**, **2^-**, **3** and **4**.

$[Pt(bzq)(C_6F_5)(CN)]^-$					
MO	**eV**	**Pt**	**bzq**	**CN^-**	**C_6F_5**
LUMO+5	3.31	3	1	0	95
LUMO+4	3.30	3	18	0	79
LUMO+3	3.16	42	10	3	46
LUMO+2	2.47	4	94	1	1
LUMO+1	1.46	3	96	1	0
LUMO	0.84	3	97	0	0
HOMO	-2.55	44	41	14	0
HOMO-1	-2.70	93	3	0	5
HOMO-2	-2.75	31	6	10	53
HOMO-3	-3.25	68	19	0	12
HOMO-4	-3.27	8	1	0	90

HOMO-5	-3.65	20	61	18	1

$[Pt(dfppy)(C_6F_5)(CN)]^-$

MO	**eV**	**Pt**	**dfppy**	**CN^-**	**C_6F_5**
LUMO+5	3.21	5	1	1	94
LUMO+4	3.21	1	7	0	92
LUMO+3	3.03	40	13	3	44
LUMO+2	2.64	13	83	3	1
LUMO+1	1.62	1	99	0	0
LUMO	0.99	5	93	1	0
HOMO	-2.82	51	32	17	0
HOMO-1	-2.87	90	4	0	7
HOMO-2	-2.91	33	4	9	54
HOMO-3	-3.35	0	0	0	99
HOMO-4	-3.42	75	21	1	3
HOMO-5	-3.70	13	84	2	1

3 (optimized model Pt_4Tl_4 based on the reported crystallographic structure)

MO	**eV**	**Pt**	**Tl**	**bzq**	**CN^-**	**C_6F_5**	**THF**
LUMO+5	-1.66	5	14	78	2	1	0
LUMO+4	-1.78	4	13	80	2	0	0
LUMO+3	-1.94	5	5	89	1	1	0
LUMO+2	-2.01	5	3	90	1	1	0
LUMO+1	-2.19	8	10	78	2	2	0
LUMO	-2.33	9	12	75	2	2	0
HOMO	-5.36	46	32	12	4	5	2
HOMO-1	-5.49	47	30	12	3	7	0
HOMO-2	-5.71	18	1	60	3	19	0
HOMO-3	-5.73	19	1	74	3	3	0
HOMO-4	-5.81	24	1	16	3	56	0
HOMO-5	-5.83	23	2	6	3	66	0

4 (optimized model Pt_4Tl_4)

MO	**eV**	**Pt**	**Tl**	**dfppy**	**CN^-**	**C_6F_5**
LUMO+5	-1.59	4	58	34	2	2
LUMO+4	-1.61	7	61	28	2	3
LUMO+3	-1.96	7	3	88	1	1
LUMO+2	-1.97	7	7	82	2	1
LUMO+1	-2.37	12	18	67	2	2
LUMO	-2.51	15	25	53	5	2
HOMO	-6.18	34	9	50	3	3
HOMO-1	-6.21	32	10	53	2	3
HOMO-2	-6.22	25	4	17	3	51
HOMO-3	-6.24	24	3	9	2	61
HOMO-4	-6.34	33	9	21	3	35
HOMO-5	-6.35	32	11	32	2	23

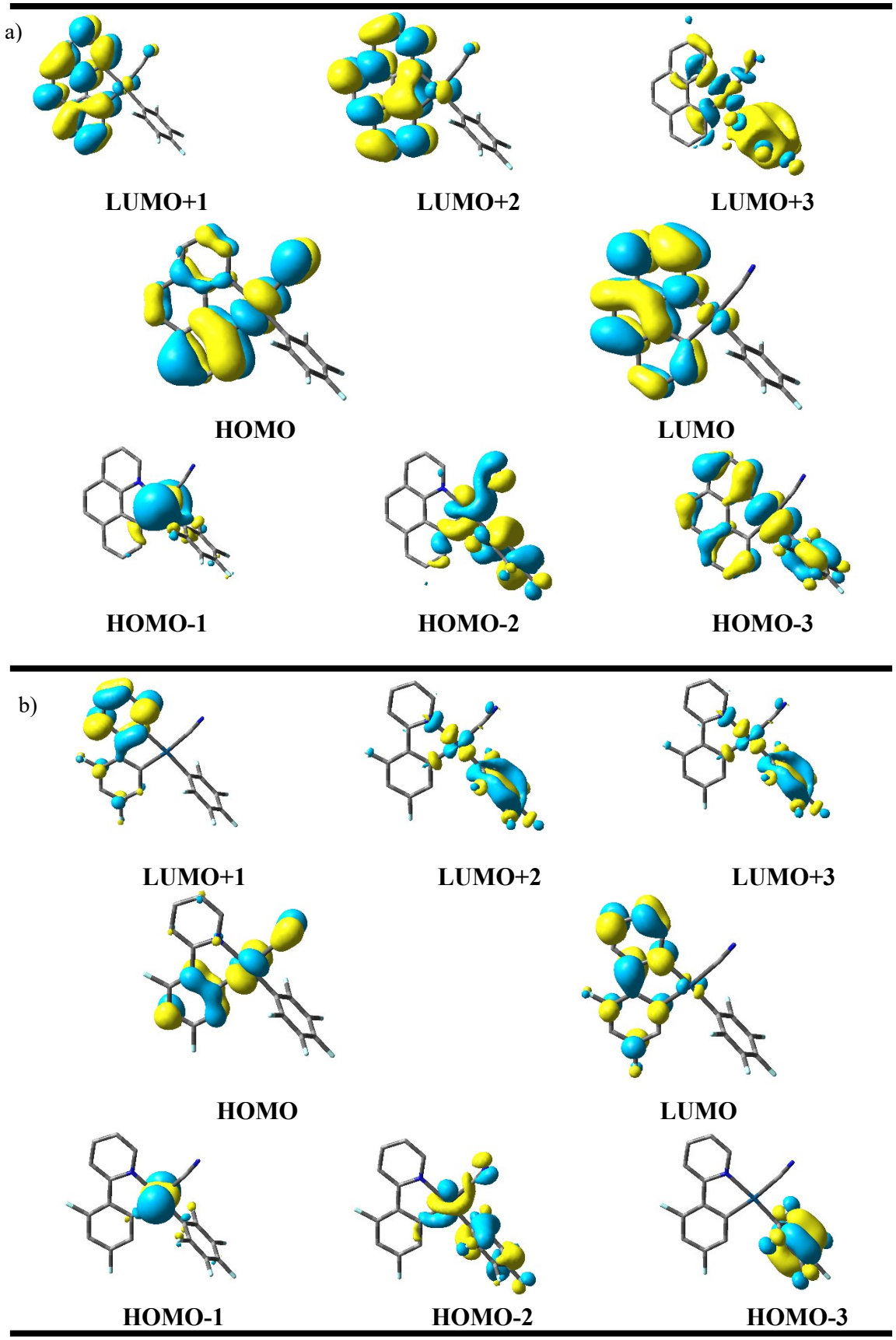

Figure S14. Selected frontier molecular orbitals for a) **1** and b) **2** and in the ground state in **solid state**.

3 (optimized model Pt_4Tl_4 based on the reported crystallographic structure)	
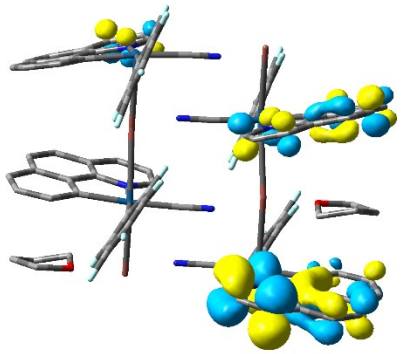	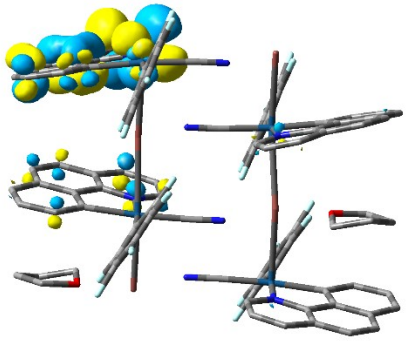
LUMO+3	**LUMO+2**
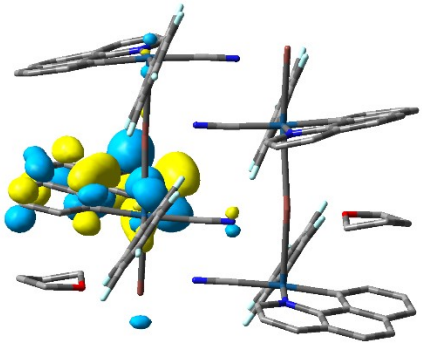	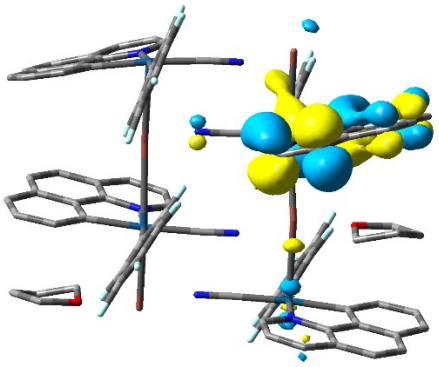
LUMO+1	**LUMO**
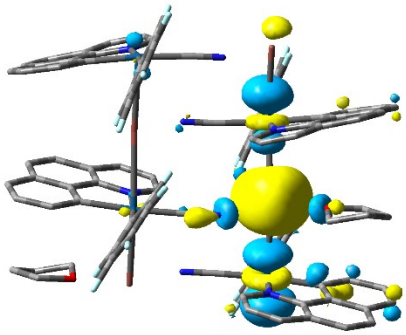	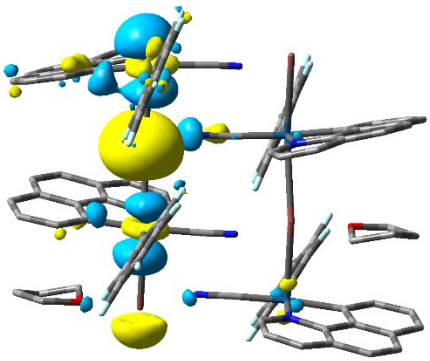
HOMO	**HOMO-1**
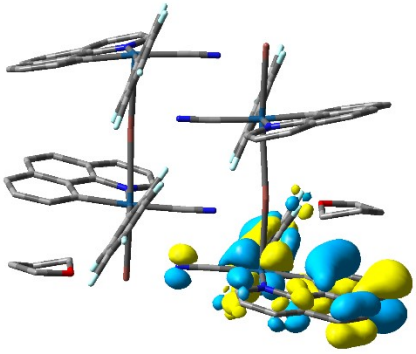	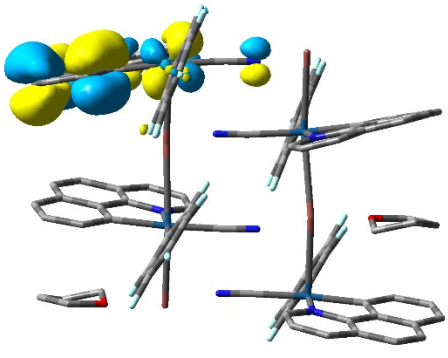
HOMO-2	**HOMO-3**

4 (optimized model Pt_4Tl_4)	
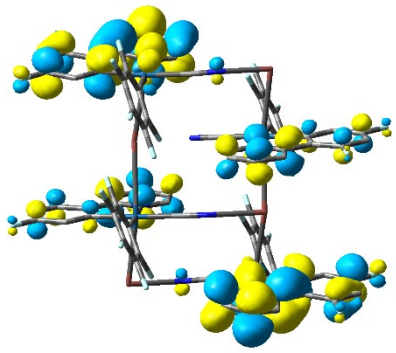	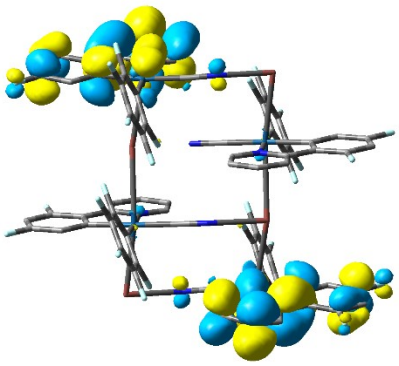
LUMO+3	**LUMO+2**
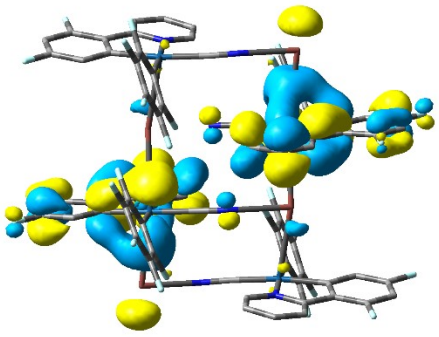	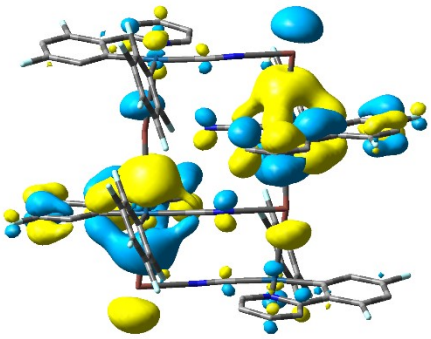
LUMO+1	**LUMO**
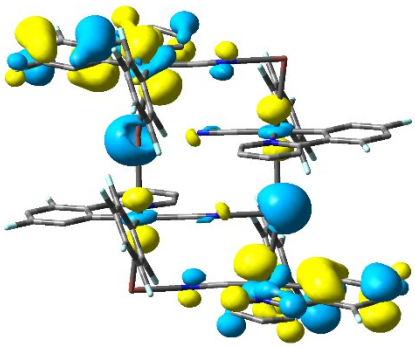	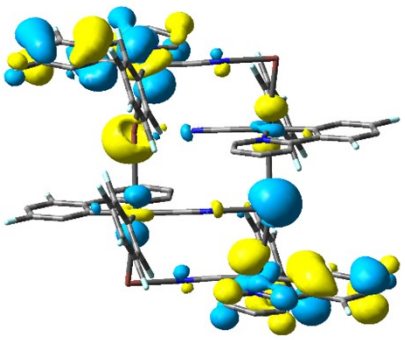
HOMO	**HOMO-1**
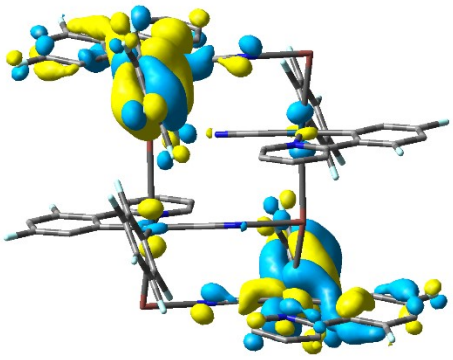	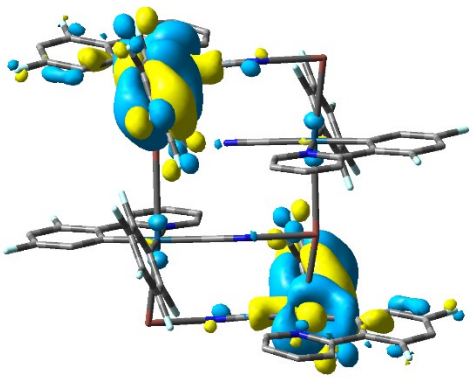
HOMO-2	**HOMO-3**

Figure S15. Plots and composition (%) of frontier MOs of the first triplet state in **solid state** for **3** and **4.**

$[Pt(bzq)(C_6F_5)(CN)]^-$ (1^-)	
SOMO	**SOMO-1**
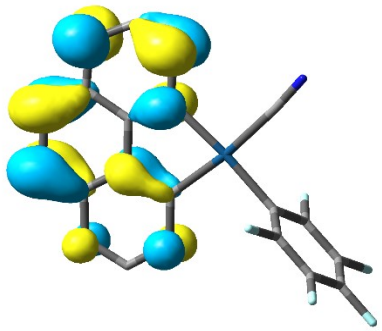	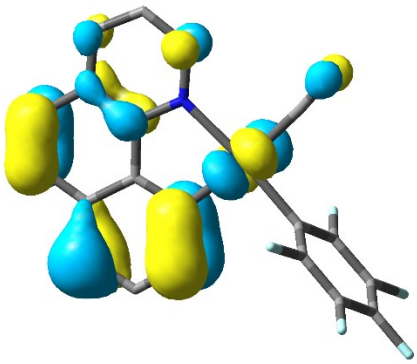
-0.40 eV	-1.46 eV
Pt 1%, bzq 99%, CN^- 0 %, C_6F_5 0%	Pt 16%, bzq 80%, CN^- 4%, C_6F_5 0%
$[Pt(dfppy)(C_6F_5)(CN)]^-$ (2^-)	
SOMO	**SOMO-1**
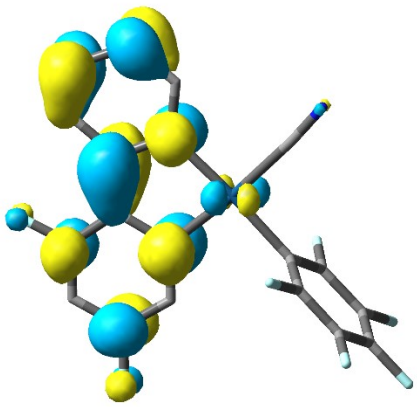	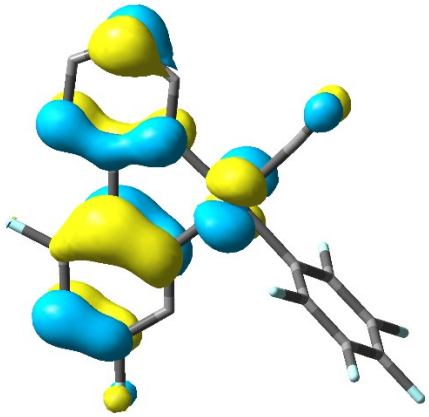
-0.50 eV	-1.64 eV
Pt 5%, dfppy 94%, CN^- 1 %, C_6F_5 0%	Pt 24%, dfppy 73%, CN^- 3%, C_6F_5 0%

$[Pt(bzq)(C_6F_5)(CN)]^-$	$[Pt(dfppy)(C_6F_5)(CN)]^-$
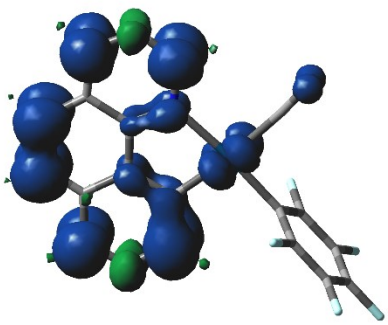	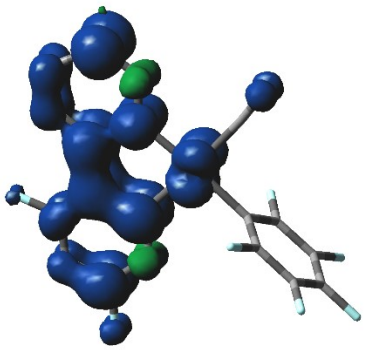
Spin density on Pt 0.163	**Spin density on Pt 0.297**

Figure S16. Plots and composition (%) of frontier MOs of the first triplet state in solid-state and spin distribution for the lowest triplet excited state for $\mathbf{1}^-$ and $\mathbf{2}^-$.

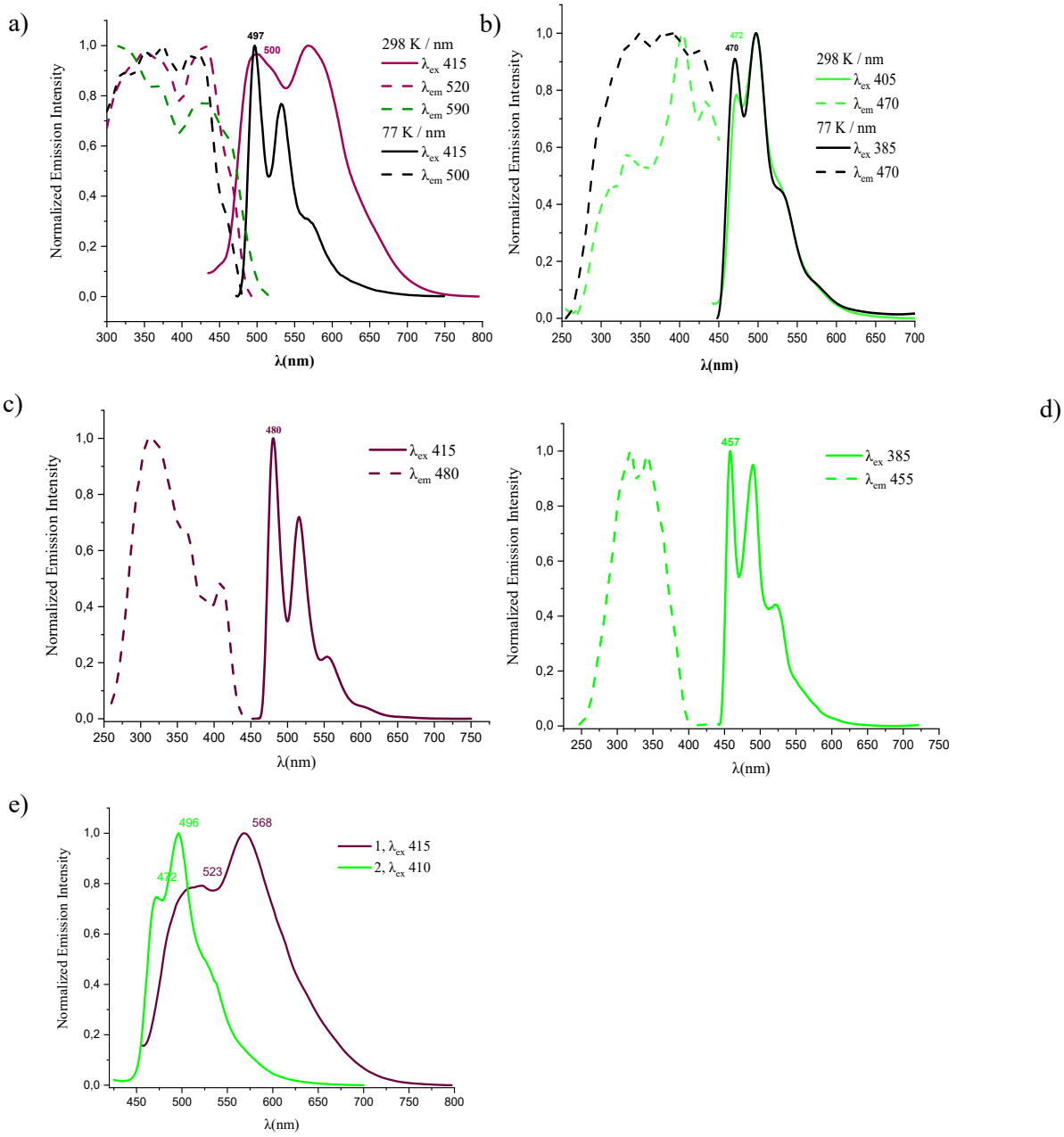

Figure S17. Normalized excitation and emission spectra of a) **1**, b) **2** in the solid state at 298 and 77 K; c) **1**, d) **2** in THF 5×10^{-5} M at 77 K; e) **1**, **2** in PS at 5% *wt* at 298 K.

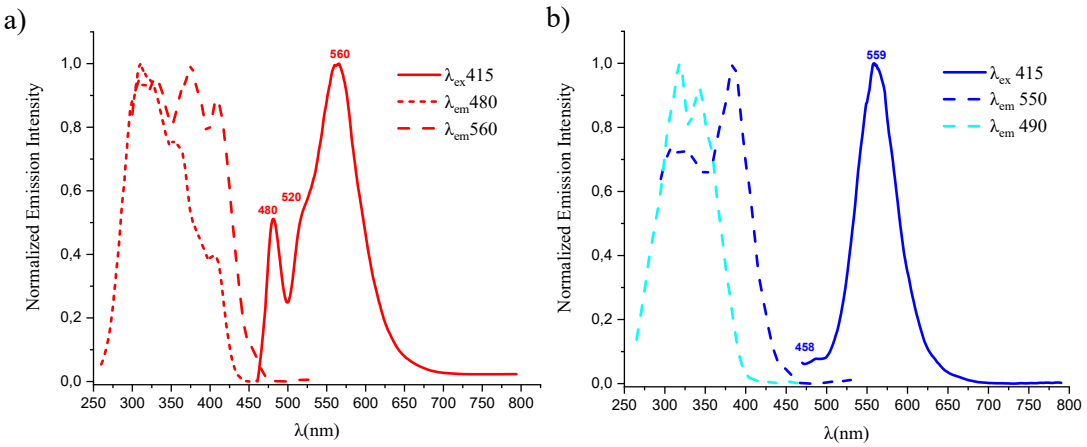

Figure S18. Normalized excitation (dashed line) and emission (solid line) spectra of a) **3**, b) **4** in THF 5×10^{-5} M at 77 K.

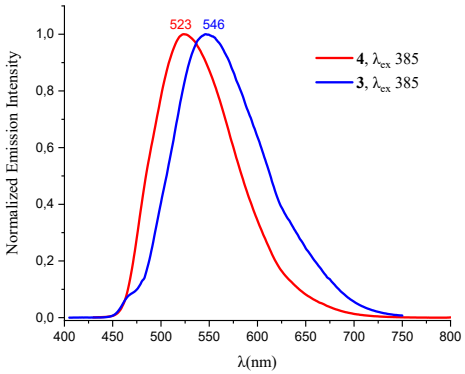

Figure S19. Normalized emission spectra of the compounds **3**, **4** in PS at 5% *wt* at 298K.

Table S10. Photoluminescence Properties of **3, 4** in Solid State, $\lambda_{em}(\lambda_{ex})$/nm

T(K)	3-Pristine	3-ground	3-MeOH	3-THF	3-Et_2O	3-CH_2Cl_2	4-Pristine	4-ground	4-MeOH
298	595(460)	606, 631_{sh}(460)	583(415)	639(405)	606(415)	558_{sh}, 632(415)	546(460)	558, 610, 642 (500)	590(460)
77	658(525)	662(525)	650(530)	709(600)	624,691 (580)	720(615)	563(450)	567, 670 (480)	662(520)

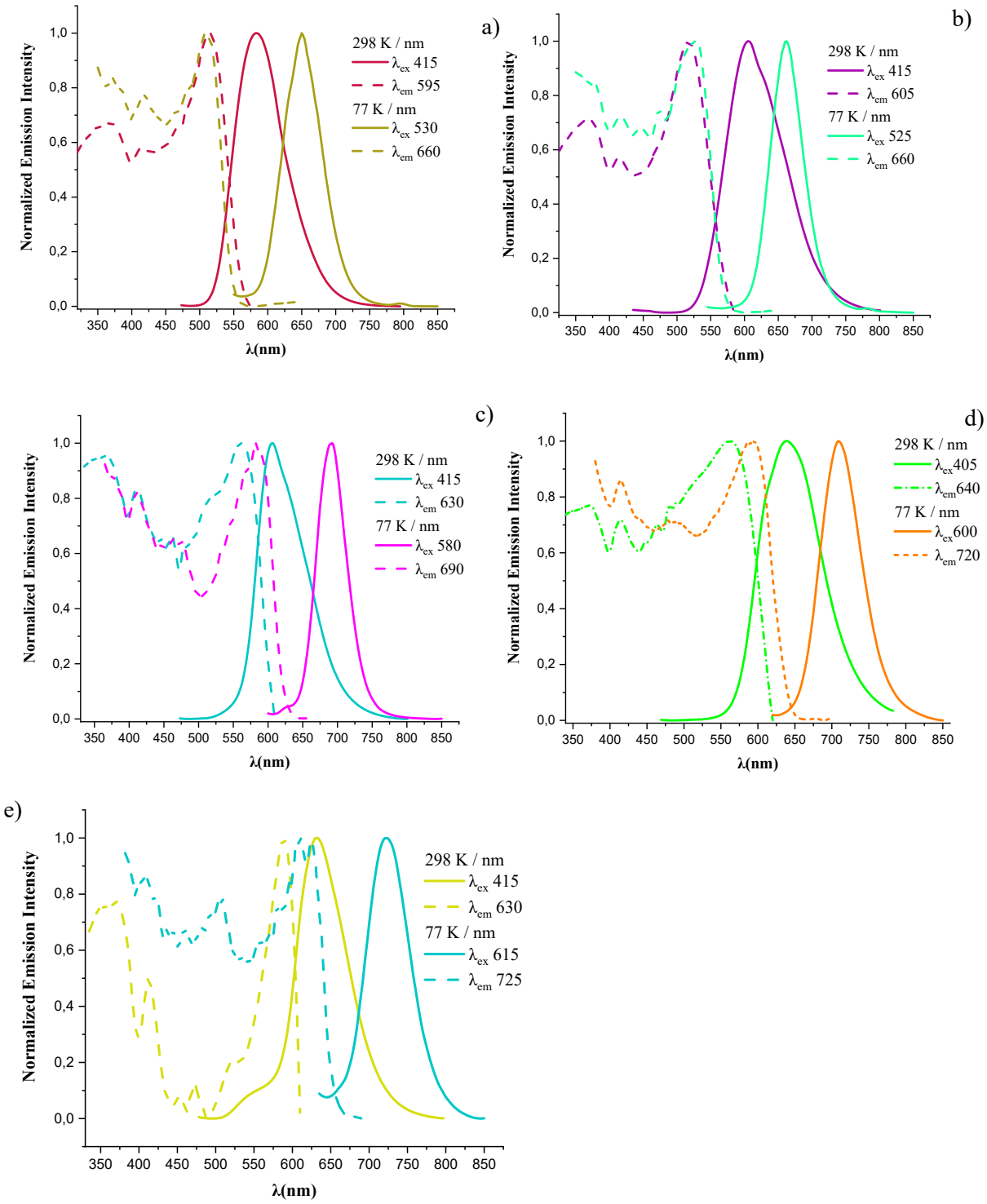

Figure S20. Normalized excitation (dashed line) and emission (solid line) spectra of complex a) **3-MeOH**, b) **3-Ground**, c) **3-Et$_2$O**, d) **3-THF**, e) **3-CH$_2$Cl$_2$** in the solid state at 298 and 77 K.

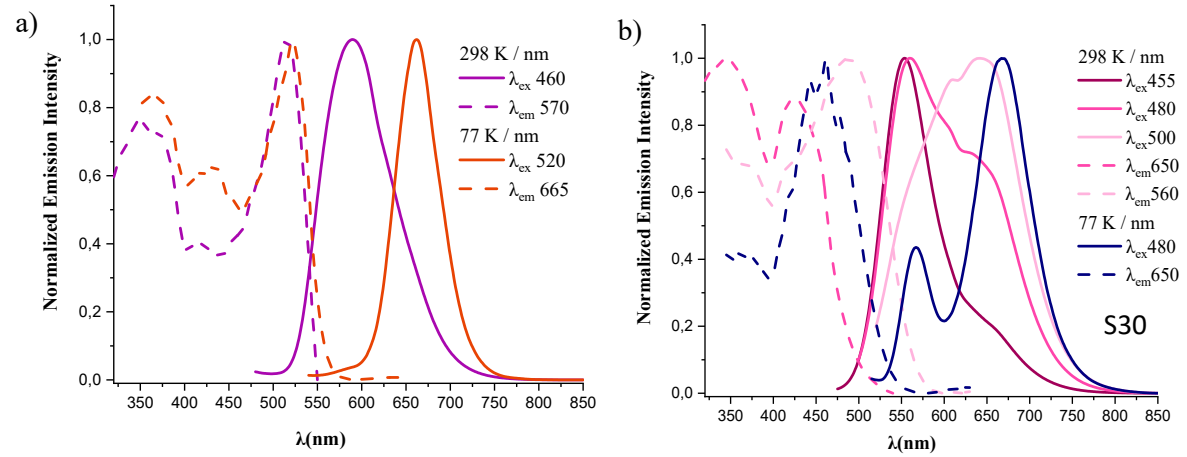

Figure S21. Normalized excitation (dashed line) and emission (solid line) spectra of complex a) **4-MeOH**, b) **4-Ground** in the solid state at 298 and 77 K.